Electronic Supplementary Material

Chemical vapor deposition growth of large-scale hexagonal boron nitride with controllable orientation

Xiuju Song[1], Junfeng Gao[3], Yufeng Nie[1], Teng Gao[1], Jingyu Sun[1], Donglin Ma[1], Qiucheng Li[1], Yubin Chen[1], Chuanhong Jin[4], Alicja Bachmatiuk[5], Mark H. Rümmeli[6,7], Feng Ding[3] (✉), Yanfeng Zhang[1,2] (✉), and Zhongfan Liu[1] (✉)

[1] *Center for Nanochemistry (CNC), Beijing Science and Engineering Center for Low Dimensional Carbon Materials, Beijing National Laboratory for Molecular Sciences, College of Chemistry and Molecular Engineering, Academy for Advanced Interdisciplinary Studies, Peking University, Beijing 100871, China*

[2] *Department of Materials Science and Engineering, College of Engineering, Peking University, Beijing 100871, China*

[3] *Institute of Textiles and Clothing, Hong Kong Polytechnic University, Hong Kong, China*

[4] *State Key Laboratory of Silicon Materials, Department of Materials Science and Engineering, Zhejiang University, Hangzhou 310027, China*

[5] *Centre of Polymer and Carbon Materials, Polish Academy of Sciences, M. Curie-Sklodowskiej 34, Zabrze 41-819, Poland*

[6] *Department of Energy Science, Department of Physics, Sungkyunkwan University, Suwon 440-746, Republic of Korea*

[7] *IBS Center for Integrated Nanostructure Physics, Institute for Basic Science (IBS), Daejon 305-701, Republic of Korea*

Supporting information to DOI 10.1007/s12274-015-0816-9

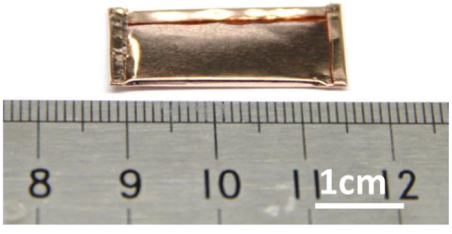

Figure S1 Photograph of a Cu enclosure.

Address correspondence to Zhongfan Liu, zfliu@pku.edu.cn; Yanfeng Zhang, yanfengzhang@pku.edu.cn; Feng Ding, feng.ding@polyu.edu.cn

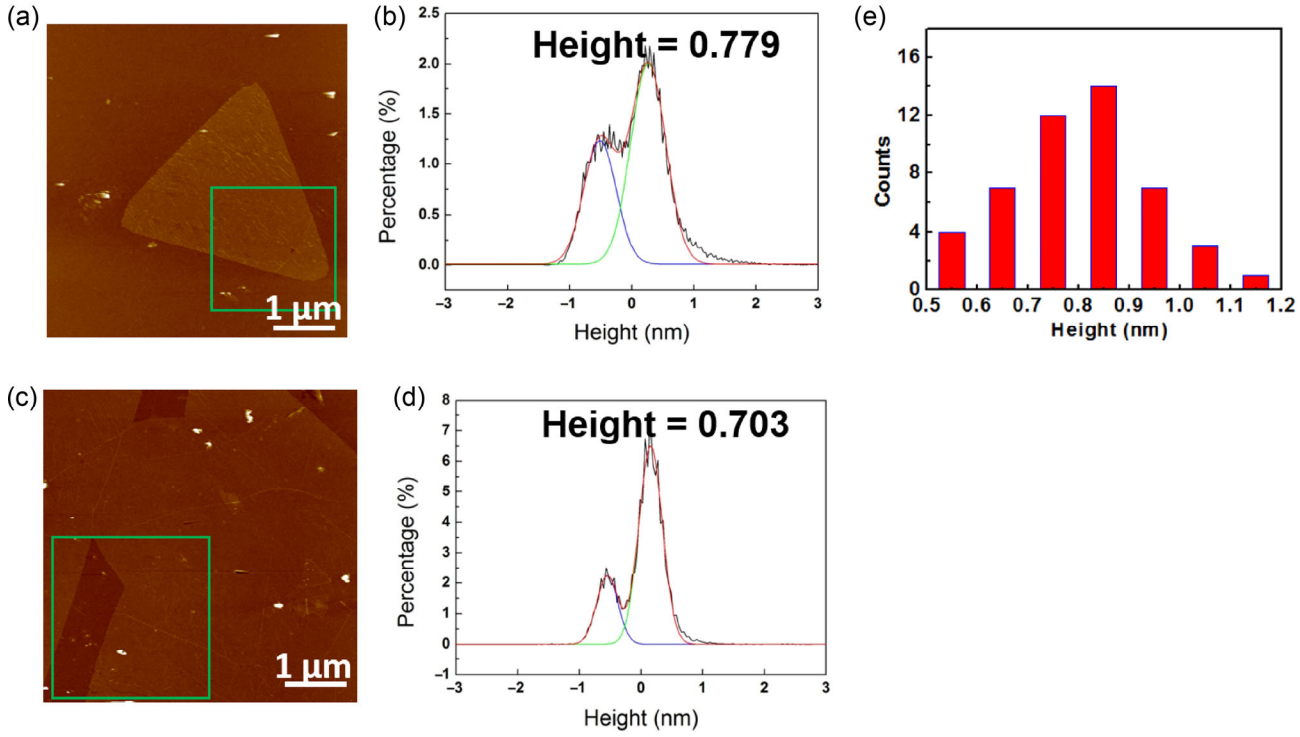

Figure S2 AFM height measurement of h-BN transferred onto SiO_2/Si. AFM images of an h-BN triangle (a) and near-fully covered h-BN film (c). (b) and (d) are the height histograms of green rectangular region in image (a) and (c), respectively. (e) Distribution of height measurement of h-BN are measured at 48 regions, showing that the thickness of 92% h-BN film is between 0.5–0.9 nm, which is consistent with the thickness of monolayer h-BN films [S1].

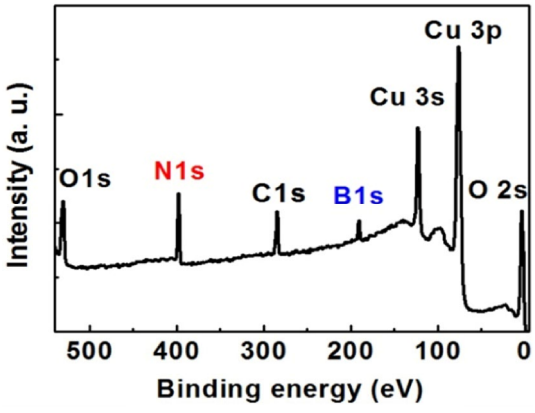

Figure S3 A survey XPS spectrum of as-grown h-BN on Cu foils. The existence of B 1s and N 1s peaks demonstrates the presence of h-BN [S2].

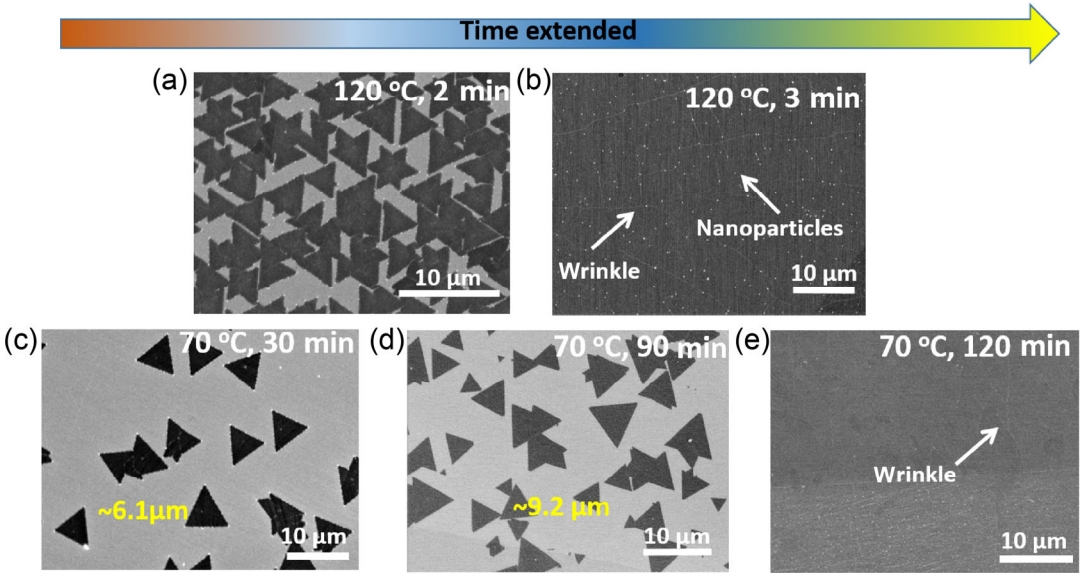

Figure S4 Time dependence of h-BN growth on Cu foils. SEM images of h-BN grown on Cu foils at different T_p temperatures and growth time: (a) 120 ˚C, 2 min; (b) 120 ˚C, 3 min; (c) 70 ˚C, 30 min; (d) 70 ˚C, 90 min; (e) 70 ˚C, 120 min.

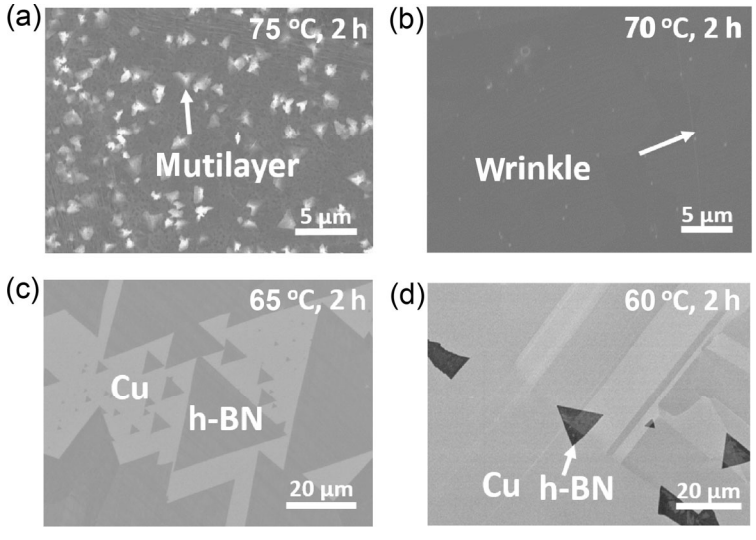

Figure S5 Precursor evaporation temperature dependence of h-BN growth on Cu foils. SEM images of h-BN grown on Cu foils for 2 h at different T_p temperatures: (a) 75, (b) 70, (c) 65, (d) 60 ˚C.

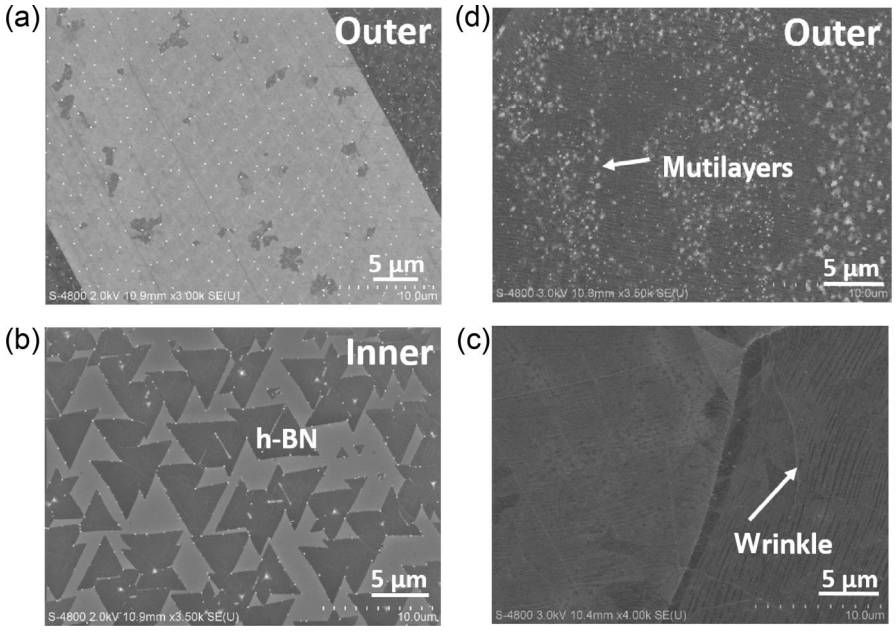

Figure S6 h-BN growth on the outer and inner surface of Cu enclosure. SEM images of h-BN grown on the outer (a) and inner surface (b) of Cu enclosure with T_p = 70 ˚C for 2 h. SEM images of h-BN grown on the inner (c) and outer surface (d) of Cu enclosure with the T_p = 100 ˚C for 3 min.

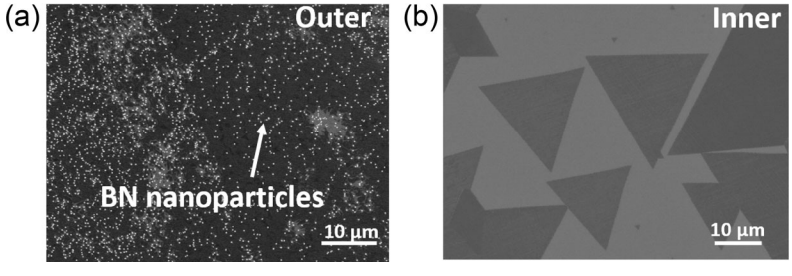

Figure S7 Contaminations on the outer surface of Cu foils. SEM images of h-BN grown on the outer (a) and inner surface (b) of Cu enclosure with T_p = 65 ˚C for 2 h. There are a numerous number of BN nanoparticles were observed on the outer surface of Cu enclosure.

DFT calculations

First-principle calculations were performed by using the DFT and plane wave pseudopotential technique, as implemented in the Vienna Ab-initio Simulation Package (VASP) [S3, S4]. Generalized gradient approximation (GGA) with the Perdew–Burke–Ernzerhof (PBE) functional [S5] was used to describe the exchange-correlation interaction.

Projector-augmented wave (PAW) method [S6] was used to describe the core electrons. The plane-wave basis kinetic energy cutoff of 400 eV and convergence criterion criteria of 10^{-4} eV were used in all the calculations. A conjugate-gradient algorithm was used to relax the ions until the force was less than 0.02 eV/Å. The partial occupancies for each wavefunction were determined by method of Methfessel-Paxton with an order of 1 and the width of the smearing is 0.2 eV. In all calculations, the Brillouin zone was sampled with dense reciprocal meshes (the separation is less than 0.2 $Å^{-1}$).

Four-row wide zigzag BN ribbon with hydrogen-terminated B edges was put on the Cu surfaces. To evaluate the interaction of h-BN edges with different orientations on Cu surface, six supercell with one co-periodic dimension of h-BN zigzag periods and Cu direction were built for BN edges on Cu (111) surface. That is 1 zigzag periodic BN edge versus 1R0° direction (in related to the lattice vectors of $[\bar{1}10]$ and $[00\bar{1}]$) of Cu subsurface (1ZZ@1R0°), 8 zigzag periodic BN edge versus $\sqrt{57}$ R6.6° (8ZZ@$\sqrt{57}$ R6.6°), and similar (8ZZ@ $3\sqrt{7}$ R19.1°), (9ZZ@$2\sqrt{19}$ R23.4°), (8ZZ@$\sqrt{61}$ R26.3°) and (7ZZ@$4\sqrt{3}$ R30.0°) with same abbreviated formation. Similar to on Cu (111), BN edges with eight orientations were sampled on Cu (100) surface, that is (1ZZ@1R0°), (7ZZ@$5\sqrt{2}$ R8.1°), (10ZZ@$3\sqrt{10}$ R18.4°), (7ZZ@$3\sqrt{5}$ R26.6°), (6ZZ@ $\sqrt{34}$ R31.0°), (5ZZ@5R36.9°), (8ZZ@$\sqrt{61}$ R39.8°), (3ZZ@ $2\sqrt{2}$ R45.0°) versus lattice vectors of $[01\bar{1}]$ and [011] of Cu (100) surface.

All the Cu surface is modeled with three layers metal slab with bottom layer fixed. In all calculations, periodic boundary conditions (PBC) are applied along all the three directions. The vacuum space larger than 10 Å is adopted between the neighboring images to eliminate their interactions.

There are three close-packed directions of the family $[\bar{1}10]$ for Cu (111) surface and two close-packed directions of the family $[01\bar{1}]$ for Cu (100) surface. The binding energy between h-BN edge with an angel θ to one close-packed direction of Cu surface was defined as

$$E(\theta) = (E_{tot} - E_{free} - E_{sub})/L$$

where E_{tot} is the total energy of BN edges on Cu surfaces, E_{free} is energy of free BN ribbons with hydrogen-terminated B edges in vacuum, spin-polarized DFT was used for free edge calculation. E_{sub} is the energy of Cu surface for each model, and L is the length of h-BN edge.

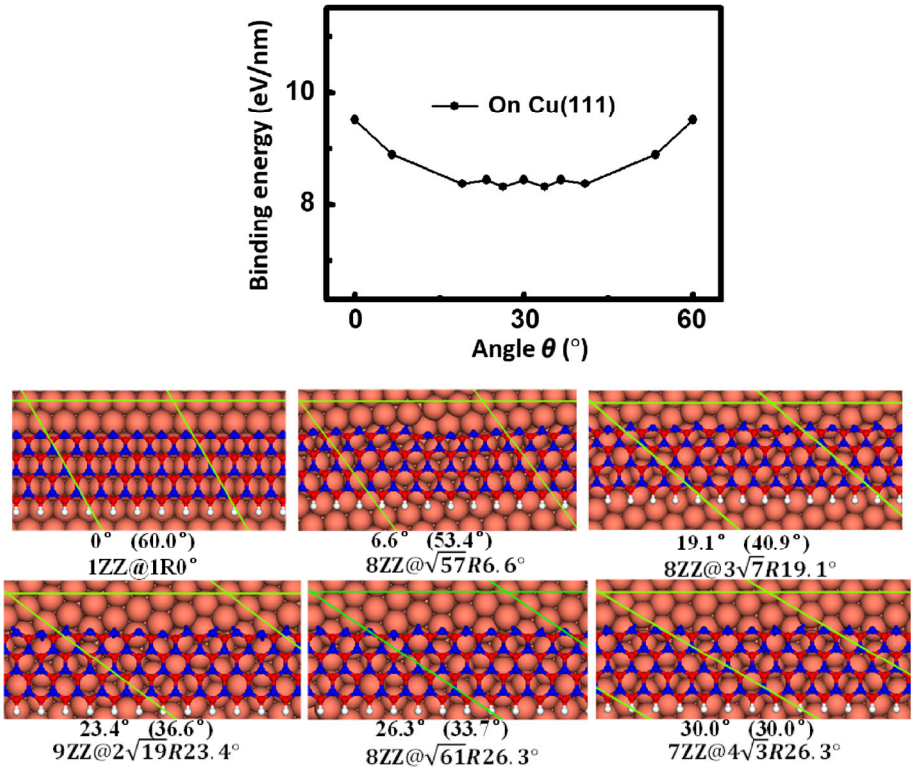

Figure S8 Binding energies of h-BN edges with different angles on Cu (111). Binding energy as a function of angle of h-BN edge to the close-packed direction on Cu (111) surface and six models of BN edges with different orientations on Cu (111) surface. Considered on top layer of Cu (111) surface, $E(\theta) = E(60° - \theta)$.

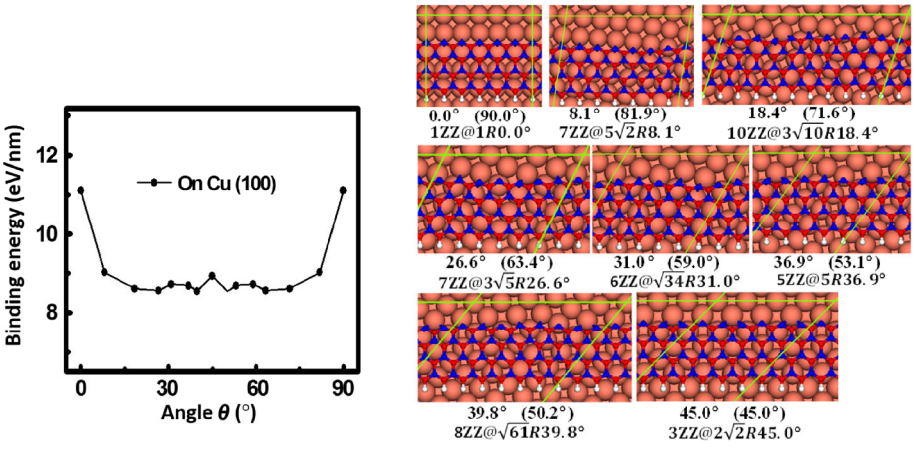

Figure S9 Binding energies of h-BN edges with different angles on Cu (100). Binding energy as a function of angle of BN edge to the close-packing direction on Cu (100) surface and eight models of h-BN edges with different orientations on Cu (100) surface. Considered on top layer of Cu (100) surface, $E(\theta) = E(90° - \theta)$.

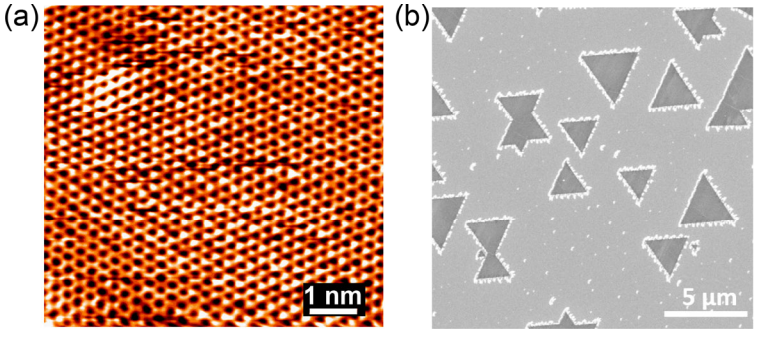

Figure S10 h-BN growth on Cu (111) single crystal. (a) Atomic-resolution STM image of h-BN lattice (VT = –0.002 V, IT = 9.498 nA). (b) SEM image of h-BN grown on Cu (111) single crystal with T_p = 75 ˚C for 20 min.

Reference

[S1] Kim, K. K.; Hsu, A.; Jia, X. T.; Kim, S. M.; Shi, Y. S.; Hofmann, M.; Nezich, D.; Rodriguez-Nieva, J. F.; Dresselhaus, M.; Palacios, T. et al. Synthesis of monolayer hexagonal boron nitride on Cu foil using chemical vapor deposition. *Nano Lett.* **2012**, *12*, 161–166.

[S2] Tay, R. Y.; Griep, M. H.; Mallick, G.; Tsang, S. H.; Singh, R. S.; Tumlin, T.; Teo, E. H.; Karna, S. P. Growth of large single-crystalline two-dimensional boron nitride hexagons on electropolished copper. *Nano Lett.* **2014**, *14*, 839–846.

[S3] Kresse, G.; Furthmüller, J. Efficiency of *ab-initio* total energy calculations for metals and semiconductors using a plane-wave basis set. *Comp. Mater. Sci.* **1996**, *6*, 15–50.

[S4] Kresse, G.; Furthmüller, J. Efficient iterative schemes for *ab initio* total-energy calculations using a plane-wave basis set. *Phys. Rev. B* **1996**, *54*, 11169–11186.

[S5] Perdew, J. P.; Burke, K.; Ernzerhof, M. Generalized gradient approximation made simple. *Phys. Rev. Lett.* **1996**, *77*, 3865–3868.

[S6] Blöchl, P. E. Projector augmented-wave method. *Phys. Rev. B* **1994**, *50*, 17953–17979.